Dichloromethane Photodegradation Using Titanium Catalysts

JAMES F. TANGUAY,* STEVEN L. SUIB,*,†,‡,[1] AND ROBERT W. COUGHLIN*,†,‡

*Department of Chemistry, †Institute of Materials Science, ‡Department of Chemical Engineering, University of Connecticut, Storrs, Connecticut 06268

The use of titanium dioxide and titanium aluminosilicates in the photocatalytic destruction of chlorinated hydrocarbons is investigated. Titanium-exchanged clays, titanium-pillared clays, and titanium dioxide in the amorphous, anatase, and rutile forms are used to photocatalytically degrade dichloromethane to hydrochloric acid and carbon dioxide. Bentonite clays pillared by titanium dioxide are observed to be more catalytically active than titanium-exchanged clays. Clays pillared by titanium aluminum polymeric cations display about the same catalytic activity as that of titanium-exchanged clays. The rutile form of titanium dioxide is the most active catalyst studied for the dichloromethane degradation reaction. The anatase form of titanium dioxide supported on carbon felt was also used as a catalyst. This material is about five times more active than titanium dioxide-pillared clays. Degradation of dichloromethane using any of these catalysts can be enhanced by oxygen enrichment of the reaction solution or by preirradiating the catalyst with light. © 1989 Academic Press, Inc.

I. INTRODUCTION

Chlorinated hydrocarbons have been found contaminating wastewater (1), lake water (2), river water (3) and fish (4) in many areas around the world. These substances are not readily degraded or hydrolyzed in an aquatic environment. Ollis and co-workers have shown that titanium dioxide can be used to completely degrade simple chlorinated hydrocarbons in the concentration range of 10–1000 ppm to CO_2 and HCl (5–9). Dichloromethane is used in the present work as a model compound to identify and study catalysts for its photodegradation.

Aluminosilicates in the form of smectic clays and pillared clays (PILCs) have been shown to be stable and selective catalysts for various photochemical reactions (10, 11). Smectite clays contain aluminosilicate layers made up of Al^{3+} cations bound to an octahedral arrangement of O^{2-} anions (12) as well as layers of SiO_4 units with silicon and oxygen atoms in a tetrahedral arrangement (13). The present work employs ben-

tonite, a clay of the montmorillonite family having the generalized formula

$$A_x(Al_{2-x})Si_4O_{10}(OH)_2,$$

where A_x represents the exchangeable cations located in the interlamellar spaces of the clays. Bentonites have an octahedral layer of (Al_{2-x}) sandwiched between two tetrahedral layers of (Si_4). The exchangeable cations located between the clay layers maintain electrical neutrality throughout the overall structure by compensating for the negative charge of the clay layers. Natural clays typically contain exchangeable magnesium, calcium, sodium, or potassium cations. Typical surface areas of montmorillonites are on the order of 80–90 m^2/g.

Inserting large cations (i.e., pillaring) between the layers of these clays expands their structure and increases their surface areas. Typical pillaring ions are poly- or oligomeric hydroxy metal cations (12, 14, 15). Since the first report of their preparation by Barrer and Macleod (40), numerous PILCs have been made using a variety of metal cations to prop apart the layers (15–23). Occelli and Tindwa, for example,

have reported that clays pillared with $\{Al_{13}O_4(OH)_{24}(H_2O)_{12}\}^{7+}$ cations expanded from a basal spacing of 13 to 18 Å upon pillaring (17). Surface areas of such pillared clays are of the order of 200–300 m²/g.

One type of pillared clay used in this study is analogous to that studied by Occelli and Tindwa who used an aluminum hydroxy polymer as the pillaring agent (17). Studies of Rausch and Bale (24) suggest that the cationic pillaring species is $\{Al_{13}O_4(OH)_{24}(H_2O)_{12}\}^{7+}$. This proposed polymeric cation contains 12 aluminum octahedra and 1 aluminum tetrahedron. Heating clays pillared by such polymeric cations causes dehydration and forms linkages between the clay layers and the Al_{13} pillars.

A second type of PILC used in this study has pillars of titania. Polymeric hydroxy titanium cations can be prepared by mixing a solution of titanium tetrachloride and hydrochloric acid (25). Heating clays containing these exchanged cations presumably forms pillars of titanium dioxide between the clay layers. The resulting material is reported (25) to be thermally stable to 500°C with a pillar height of 13.5 Å and a surface area of 300 m²/g. The unit cell formula is reported (25) to be $(TiO_2)_{7.0}$ $\{Si_{7.78}Al_{0.22})(Al_{3.20}Mg_{0.64}Fe_{0.16})\}O_{20}(OH)_4$.

Titanium dioxide is also prepared by sol-gel techniques (26) and used as a catalyst in this work. This titania can be amorphous or crystalline (anatase or rutile) depending on preparation and treatment. These titania catalysts are synthesized and deposited on inert supports of carbon felt. In this way supported titania of high surface area and small particle size can be used as a catalyst that is easily separated from the reaction solution.

Below we report photocatalytic activities and deactivation behavior of various preparations of titanium aluminosilicates and supported titania. The catalysts are characterized by X-ray diffraction, BET surface area measurements, and electron paramagnetic resonance (EPR) spectroscopy. Two types of titania-pillared clays show a high catalytic activity for dichloromethane degradation.

II. EXPERIMENTAL

A. Titanium Exchange of Clays

A bentonite clay of low iron content termed Bentolite L (Lot No. 6-86062401-50305) was obtained from Southern Clay Products, a subsidiary of E.C.C. America, Inc. (Gonzales, TX). Clays were ion exchanged with solutions of TiI_4 in distilled deionized water at starting concentrations ranging from 0.01 to 0.7 M. A 5.0-g portion of Bentolite L was mixed with 500 ml of the TiI_4 solution and stirred for 24 h at room temperature. The solid product was filtered with a fritted funnel of fine porosity, washed with three 100-ml aliquots of distilled deionized water, and dried at 100°C for 6 h. All samples contain about 10 mmol titanium/g of clay.

B. Titanium–Aluminum Chlorohydroxyl (ACH) Pillared Clays

Bentolite L clays were pillared with an ACH solution (Lot No. 7698) obtained from the Reheis Chemical Co. (Berkeley Heights, NJ). The pillaring solution, prepared by mixing 2.83 g of TiI_4 with 6.5 ml of ACH, was first slowly stirred at room temperature for 12 h. This solution was then added dropwise to a suspension of 5.0 g of Bentolite L in 500 ml of distilled, deionized water and the resulting mixture stirred at 70°C for 2 h. The solid product was then filtered, washed, and dried for 12 h as described above.

C. Titania–Pillared Clays

The pillaring solution, a mixture of 5 ml of $TiCl_4$ (Lot No. B05G from Alfa Ventron, Danvers, MA) and 10 ml of 6 M HCl, was diluted to a total volume of 61 ml with distilled, deionized water then stirred at room temperature for 5 h. The solution was then added to a suspension of 5.0 g of Bentolite L in 1250 ml of distilled, deion-

ized water and the resulting mixture stirred at room temperature for 18 h. The pillared solid was filtered and washed with distilled, deionized water until the washings were negative to a silver nitrate test for Cl^-. The product was air-dried at 260°C for 10 h.

D. Titania Preparation

Titania was prepared following the sol-gel technique described by Wright and co-workers (26). A solution containing 36 ml of water was mixed with 2 ml of an isopropa-nol (Lot No. 949840, Baker Chemical, Phillipsburg, NJ) solution containing 2.0×10^{-3} mol of HNO_3. This solution was added dropwise to 20 ml of titanium isopropoxide (Lot No. E14G, Alfa Ventron, Danvers, MA), and the resulting mixture was allowed to stand at room temperature for 14 h. Over this period of time a white gelatinous precipitate slowly formed. The solid was washed with three 25-ml aliquots of a 1 ml/10 ml mixture of isopropanol and water. The gel was air-dried at 70°C for 12 h. At this point the material was amorphous and displayed no X-ray diffraction pattern. The solid was heated to 375°C for 12 h in air to obtain the anatase structure or to 850°C for 12 h in air to obtain the rutile structure.

E. Titania Preparation on Carbon Felt

Carbon felt (4 × 4 × 0.5 cm) was saturated with a solution attained by mixing a solution of 36 ml of water with 2 ml of an isopropanol solution containing 2×10^{-3} mol of HNO_3. Approximately 5 ml of titanium isopropoxide was dropped on one side of the felt. During the next 14 h at room temperature, titania formed within the felt and as a thin film and on its surface. The felt was then washed with 50 ml of distilled, deionized water and dried at 70°C for 12 h. To obtain supported crystalline anatase on the treated felt, the material was heated to 375°C in air for 12 h.

F. X-Ray Diffraction Methods

X-ray diffraction patterns were obtained using a DIANO-8000 or a Norelco Model 67A diffractometer using nickel-filtered $CuK\alpha$ radiation. The Bragg angle was scanned at a rate of 1°/min. Diffractograms were obtained for powders mounted on glass slides lightly coated with a layer of petroleum jelly. First-order basal spacings were calculated using Bragg's law and $CuK\alpha$ ($\lambda = 1.54051$ Å) radiation.

G. Electron Paramagnetic Resonance Spectroscopy

All EPR spectra were obtained using an E3 X-band spectrometer (Varian Instruments, Union, NJ). The first derivative of absorption was recorded at 77 K. The cavity was tuned to a Klystron operating at 9150 MHz. Spectra were calibrated to a standard of 2,2'-diphenyl-1-picrylhydrazyl. Samples for measurements were sealed into 3-mm-i.d. quartz tubes under a vacuum of better than 1×10^{-4} Torr.

H. Surface Area Measurements

Surface area measurements were made on a modified Quantasorb instrument (Quantachrome Co., Syosett, NY). Surface areas were computed using the BET equation applied to three data points corresponding to mixtures of nitrogen and helium gas at relative pressures of 0.1, 0.15, and 0.2, respectively. All gases were passed through CuO_x, MnO_x, and 13X molecular sieve traps before contacting the samples previously outgassed for 12 h at 300°C in helium.

I. Chloride Ion Determination

Using the Mohr titration method, chloride ions in solution were precipitated by standardized silver nitrate in the presence of a small amount of chromate ion used as an indicator (27). Triplicate assays were made of 1-ml aliquots of the photocatalytic reaction solution. For further details see Ref. (39).

J. Catalytic Reaction Studies

A 1.5-g portion of powder catalyst or one piece of titania–carbon felt was put in a 3-neck round bottom flask with 75 ml of

dichloromethane (Lot No. KPNM, Mallinckrodt, Paris, KY) solution (CH_2Cl_2/ H_2O = 1 ml/100 ml). The flask was irradiated by a Kratos Model LH-51 1000 W continuous output xenon arc lamp and stirred magnetically throughout the reaction. Wavelengths below 300 nm were filtered from the incident light to prevent any homogeneous decomposition of the dichloromethane. The incident light intensity was not measured but settings of 34 A and 22 V were used on the lamp power supply. A Corning (7) pH meter was used to monitor the pH of the reaction.

III. RESULTS

A. Clay and Pillared Clay X-Ray Diffraction

Exchanging titanium into Bentolite L slightly reduces the first-order basal spacing from 15.5 to 13.2 Å. This is also accompanied by a reduction in the intensity of the diffraction peaks which may be attributed to attack by the acidic TiI_4 exchange solution. First-order basal spacings for all these clay materials are listed in Table 1. Upon pillaring with titanium-loaded ACH, the first-order basal spacing increases to 17.7 Å which is close to the value previously reported for ACH-pillared clays with no titanium (17). Clays pillared with titania

TABLE 1

BET Surface Areas and First-Order Basal Spacings of Clays and Pillared Clays

Sample	Surface area (m^2/g)	d_{001} (Å)
Bentolite L clay	90	15.5
Ti-exchanged Bentolite L	100	13.2
TiACH-pillared clay	129	17.7
TiO$_2$-pillared clay	229	18.6
TiO$_2$ (J. T. Baker)	59	a
Amorphous TiO$_2$	159	a
Anatase TiO$_2$	133	a
Rutile TiO$_2$	23	a

Note. a, Not applicable.

have an even larger first-order basal spacing of 18.6 Å.

B. Synthetic Titania X-Ray Diffraction

Heating the amorphous sol–gel preparation (whether an unsupported powder or supported on the carbon felt) to 375°C for 12 h in air produces a white crystalline material identified as anatase according to the ASTM standard powder diffraction files. The material appears to have no impurities revealed by X-ray diffraction. Heating anatase or the amorphous solid to 850°C for 12 h in air produces rutile as confirmed by the ASTM standard powder diffraction files. This material also appears to have no crystalline impurities.

C. Surface Area Measurements

Unexchanged Bentolite L has a surface area of 90 m^2/g. Upon titanium exchange into Bentolite L the surface area increases from 90 to 100 m^2/g. Pillaring the clay with titanium-loaded ACH raises the surface area to 129 m^2/g. Pillaring the clay with titania increases the surface area even more to 229 m^2/g. Increases in surface areas by exchange or pillaring correlates well with interlamellar distances indicated by X-ray diffraction.

Anatase purchased from the J. T. Baker Chemical Co. (Lot No. 8399) has a surface area of 59 m^2/g. Amorphous titania synthesized by us has a surface area of 159 m^2/g. Heating to convert this latter material to anatase reduces its surface area to 133 m^2/g. Further thermal conversion to the rutile form dramatically reduces the surface area to 23 m^2/g. These surface areas are summarized in Table 1.

D. EPR Studies

Titanium clays, pillared clays, and synthetic titania samples were investigated by EPR at 77 K. All samples produced a signal having g_1 = 2.015, g_2 = 2.003, and g_3 = 1.988. This spectrum is shown in Fig. 1.
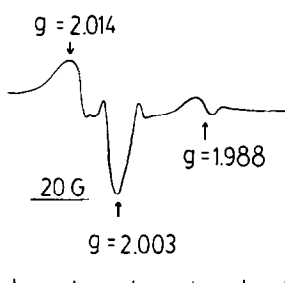
FIG. 1. EPR spectrum of titanium-pillared clays and titanium dioxide.

The EPR spectra showed no change after catalysis.

E. Titanium-Exchanged Clay Photocatalysis

The time courses of the batch photolysis reactions of CH_2Cl_2 catalyzed by titanium-exchanged Bentolite L are displayed in Fig. 2 as chloride ion concentrations plotted versus time. A direct relationship is evident between the amount of titanium loading and the extent of reaction although none of the exchanged clays are more catalytically ac-

tive than purchased titanium dioxide. Hydrogen ion production during the reaction as indicated by pH changes is summarized in Fig. 3. A correlation appears to exist between the decrease in pH and the chloride ion production. A similar pH change with time is seen in reactions catalyzed by exchanged clays and unmodified clays as well as uncatalyzed reactions caused by photolysis of solutions alone.

A very simplified kinetic model to help in data interpretation can be constructed by assuming that the reaction is irreversible and first-order in CH_2Cl_2 and poisoned by chloride ions according to

rate (mol/time-mass cat)

$$= kC_{CD}(1 - q/q_0), \quad (1)$$

where k is the first-order, specific rate constant, C_{CD} is the concentration of CH_2Cl_2, q is the concentration of poisoned sites per unit mass of catalyst, and q_0 is the total concentration of sites per unit mass of catalyst.

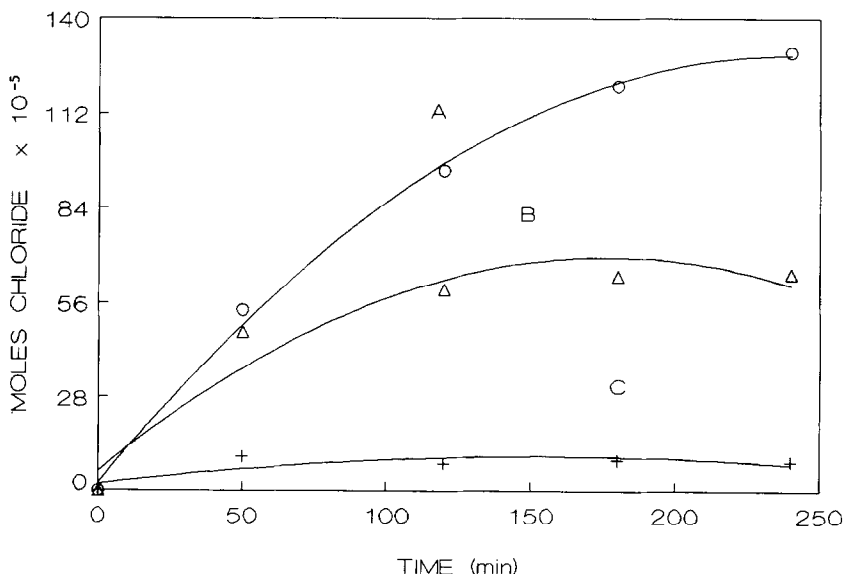If a linear relationship, $q = KC_{Cl}$, exists

FIG. 2. Chloride ion production in 100 ml of a 10,000 ppm dichloromethane solution using 1.5 g of catalysts. (A) Titanium-exchanged Bentolite L; 25 mmol Ti/g clay. (B) Titanium-exchanged Bentolite L; 10 mmol Ti/g clay. (C) Bentolite L.
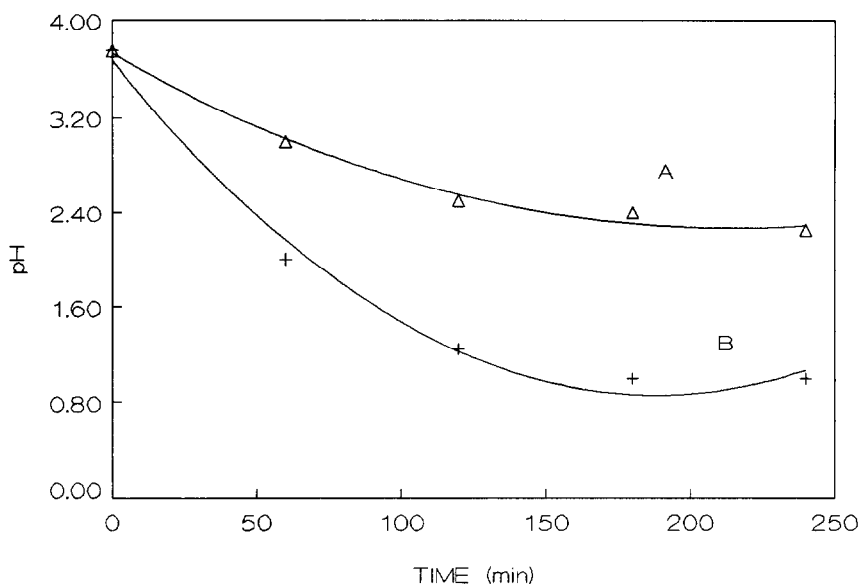
FIG. 3. The pH changes in 100 ml of a 10,000 ppm dichloromethane solution using 1.5 g of catalysts. (A) Titanium-exchanged Bentolite L; 10 mmol Ti/g clay. (B) Titanium-exchanged Bentolite L; 25 mmol Ti/g clay.

between q and chloride ion concentration, C_{Cl}, and assuming the amount of adsorbed Cl^- is negligible compared to the amount in solution, then the rate can be written as

$$\text{rate} = kC_{CD}[1 - \propto(C^\circ_{CD} - C_{CD})], \quad (2)$$

with $\propto = K/q_0$ and $(C^\circ_{CD} - C_{CD})$ substituted for C_{Cl} by stoichiometry for a batch reaction with C°_{CD} the initial concentration of CH_2Cl_2. Then the differential equation describing the time course of C_{CD} is

$$-V[dC_{CD}/dt]$$
$$= M_{cat}kC_{CD}[1 - \propto(C^\circ_{CD} - C_{CD})], \quad (3)$$

where t is the time, V is the volume of the reaction mixture, and M_{cat} is the mass of catalyst in the mixture. Inspection of the foregoing differential equation reveals that initially, when $C_{CD} = C^\circ_{CD}$,

$$k = -[dC_{CD}/dt]_{initial}/C^\circ_{CD}(M_{cat}/V) \quad (4)$$

$$k = +[dC_{Cl}/dt]_{initial}/C^\circ_{CD}(M_{cat}/V) \quad (5)$$

or that k is proportional to the initial rate of change of concentration $[dC_{Cl}/dt]_{initial}$. In addition, the reaction levels off and stops when C_{CD} falls to a value which makes $[1 - \propto(C^\circ_{CD} - C_{CD})] = 0$ or $C_{Cl,f} = C^\circ_{CD} - C_{CD} = 1/\propto$.

Thus, the final level of chloride ion attained after the reaction stops is proportional to the ratio q_0/K which is a measure of the specific number of sites on the catalyst and its resistance to deactivation by adsorbed chloride ions.

F. Titanium-Pillared Clay Photocatalysis

Chloride ion production by batch photocatalytic decomposition of dichloromethane using pillared clays is shown in Fig. 4. Titania-pillared clay is more catalytically active than TiACH-pillared clay. ACH-pillared clay is least active. The pattern of pH change during the reaction is very similar to that observed for the unpillared clay catalysts.

G. Titania-Pillared Clay Preirradiation

Reaction rates photocatalyzed by titania-pillared clays preirradiated in water for different times before addition of dichlo-
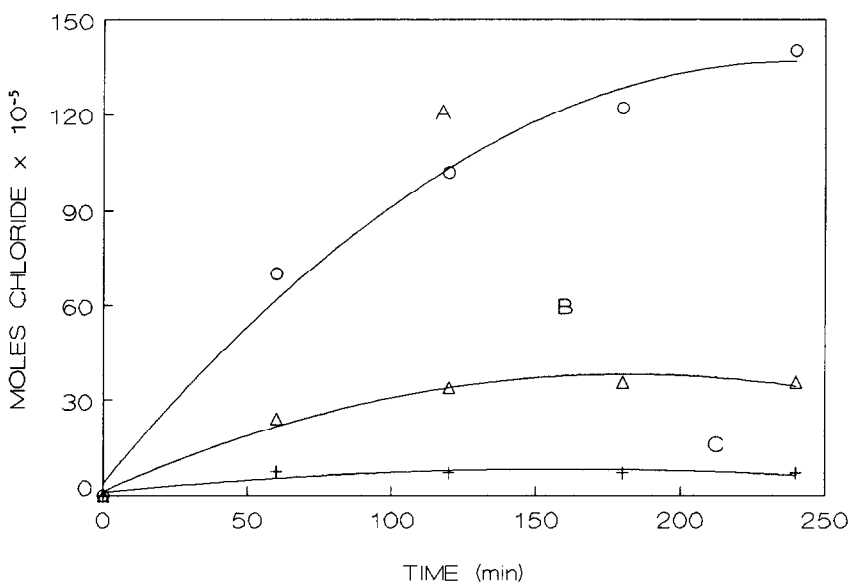
FIG. 4. Chloride ion production in 100 ml of a 10,000 ppm dichloromethane solution using 1.5 g of catalysts. (A) TiO$_2$-pillared clay; 10 mmol Ti/g clay. (B) TiACH-pillared clay; 10 mmol Ti/g clay. (C) ACH-pillared clay.

romethane are summarized in Table 2. Here initial rates are expressed per gram of catalyst as well as per unit catalyst surface area. The final chloride ion concentration in solution $C_{Cl,f}$, which is a measure of resistance to deactivation, is also listed in Table 2. It is evident that preirradiation produces only slight changes in catalytic activity or in $C_{Cl,f}$.

H. Oxygen Treatment of Titania-Pillared Clays

Figure 5 shows that bubbling oxygen gas through the reaction mixture may have a small positive effect on the photocatalytic decomposition of dichloromethane. With each catalyst the initial rate was 4.4×10^{-6} mol/min · g. With both catalysts final chloride ion concentrations greater than 1.1×10^{-3} M are attained.

I. Synthetic Titania Photocatalysis

i. Crystalline phase comparison. Figure 6 summarizes the results of chloride ion production for amorphous titania as well as the anatase and rutile phases. Amorphous

titania has little photocatalytic activity and completely deactivates after 180 min of reaction. The purchased anatase form of titania is slightly more catalytically active and more resistant to deactivation (higher $C_{Cl,f}$) than the synthetic amorphous catalyst. Synthetic anatase is also more catalytically active than the purchased anatase. Synthetic rutile is the most active catalyst and much more resistant to deactivation anatase. Kinetic data for these catalysts are summarized in Table 2.

ii. Oxygen and nitrogen treatments of synthetic titania. Table 2 summarizes the kinetic data obtained while bubbling nitrogen and oxygen separately into the reaction solution. Bubbling oxygen through the reaction mixture increases the rate of photocatalytic activity of the catalyst by about 45% and retards deactivation. Bubbling nitrogen decreases the activity, probably by removing oxygen from the reaction solution. This affirms the fact that oxygen plays an important role in dichloromethane degradation (6).

iii. Preirradiation of synthetic titania

TABLE 2

Kinetic Data of Various Forms of Supported and
Nonsupported Titania

Catalyst	Initial rate $(mol\ Cl^-\ min \cdot m^2)$	Final concentration[a] $C_{Cl,f}$ (mM)
Anatase titania on felt	1.5×10^{-7}	45
Amorphous titania on felt	6.9×10^{-8}	10
Unsupported anatase powder	1.1×10^{-7}	57
Unsupported rutile powder	1.6×10^{-6}	92
Poisoned anatase on felt	1.2×10^{-7}	18
Synthetic anatase pH 4	3.8×10^{-7}	57
Synthetic anatase pH 7	3.3×10^{-8}	14
Synthetic anatase pH 10	5.0×10^{-8}	12
Amorphous titania	1.1×10^{-7}	24
Anatase	4.1×10^{-7}	57
Rutile	2.8×10^{-6}	87
Synthetic rutile no gas bubbled	5.6×10^{-6}	92
Synthetic rutile + oxygen bubbling	1.0×10^{-5}	130
Synthetic rutile + nitrogen bubbling	2.4×10^{-6}	64
Synthetic rutile no preirradiation	5.6×10^{-6}	92
Synthetic rutile 1-h preirradiation	1.0×10^{-5}	120
Synthetic rutile 2-h preirradiation	7.0×10^{-6}	68
TiO$_2$PILC no preirradiation	3.3×10^{-8}	>14
TiO$_2$PILC 1-h preirradiation	3.8×10^{-8}	>16
TiO$_2$PILC 2-h preirradiation	3.7×10^{-8}	>4

[a] $C_{Cl,f}$, concentration of chloride ion, mmol/liter, after 240 min of reaction (end of experiment).

catalysts. Table 2 shows that preirradiating synthetic rutile catalysts increases catalytic reaction rates. Preirradiation for 60 min also appears to retard catalyst deactivation. Preirradiation for 120 min appears to counteract some of the benefits of shorter periods of preirradiation.

iv. The pH control of dichloromethane solution. Table 2 compares the catalytic performance of synthetic anatase at three different pH values. Higher reaction rates and lower deactivation occurs at the lowest pH 4.

v. Reusability and poisoning of synthetic

titania. Figure 7 shows the effect of adding 1.2×10^{-2} mol of NaCl to the initial reaction mixture. Poisoning of synthetic rutile by chloride ions is clearly evident here. Similar deactivation was observed for freshly synthesized rutile and rutile that had been used once for 240 min then washed and reintroduced into a fresh dichloromethane solution of identical starting concentration.

J. Photocatalytic Studies of Titania–Carbon Felt

When supported on carbon felt, amorphous TiO$_2$ is about as active as unsupported anatase as seen from Table 2. The results differ from those for unsupported TiO$_2$ which is less active than anatase (Table 2). Longer experiments indicate that anatase does not show significant deactivation until after about 500 min of reaction. Carbon felt with no supported titania shows about one-tenth of the activity of amorphous titania, about equal to the uncatalyzed homogeneous decomposition of dichloromethane.

Table 2 also summarizes the results of sodium chloride poisoning. These results indicate complete deactivation of the catalyst after exposure to concentrations of 18 mM of chloride ion. The initial rate for the poisoned reaction is also significantly lower than that for the unpoisoned solution.

IV. DISCUSSION

A. X-Ray Diffraction of Clays and Pillared Clays

The Bentolite L used in this work is essentially pure montmorillonite clay except for about 10% of cristobalite, a nonclay impurity (28). Upon ion exchange with TiI$_4$, all of the diffraction peaks of the clay decrease in intensity and broaden, probably due to the high acidity (pH < 2) of the exchange solution which is known to decompose zeolite lattices (29). The data in Table 1 indicate that the d_{001} spacing of the clay also decreases upon ion exchange.
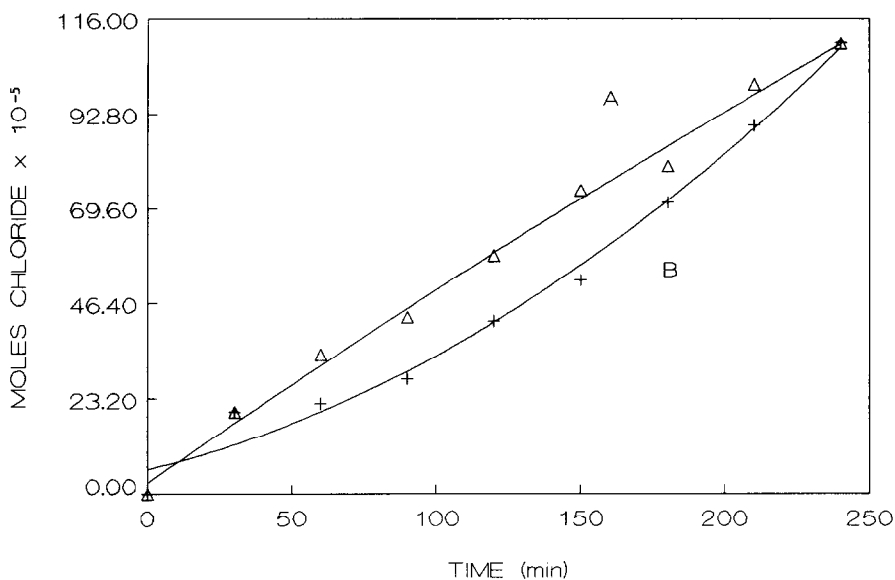
FIG. 5. Chloride ion production in 100 ml of a 10,000 ppm dichloromethane solution using 1.5 g of catalysts. (A) TiO₂-pillared clay; 10 mmol Ti/g clay, 100 ml/min oxygen bubbling. (B) TiO₂-pillared clay; 10 mmol Ti/g clay, no oxygen bubbling.

This can also be attributed to loss of water of hydration or lattice decomposition which would allow a smaller coordination of water around titanium, as previously proposed for Fe^{3+} and Cr^{3+} clays and pillared clays (19).

Pillaring the clays leads to an increase in the d_{001} spacing ranging from about 15.5 Å
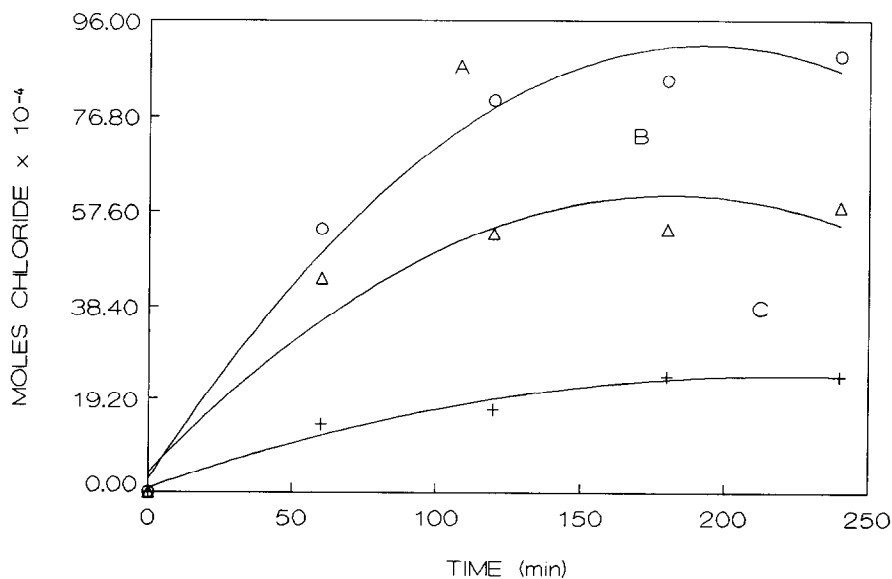

FIG. 6. Chloride ion production in 100 ml of a 10,000 ppm dichloromethane solution using 1.5 g of catalysts. (A) Rutile titania. (B) Anatase titania. (C) Amorphous titania.
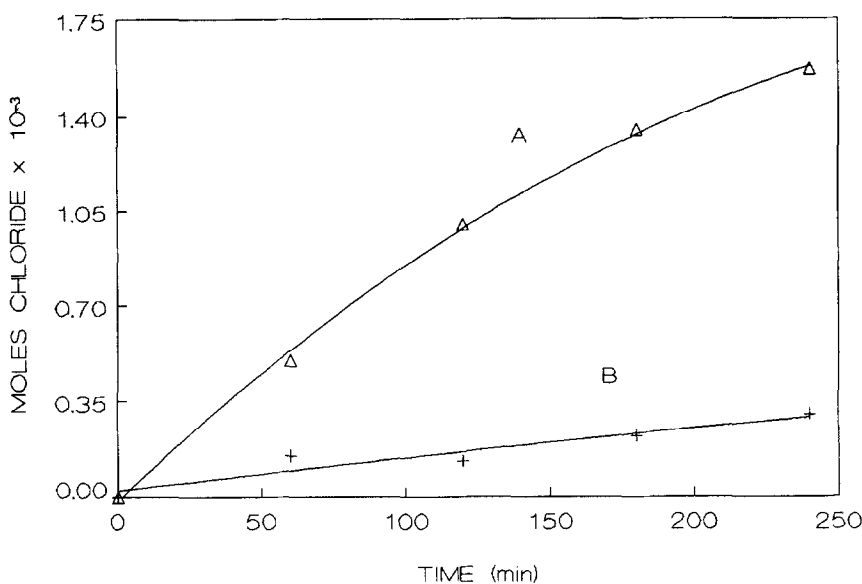
FIG. 7. Chloride ion production using 1.5 g of rutile titania in 100 ml of (A) 10,000 ppm dichloromethane solution; (B) 10,000 ppm dichloromethane solution + 0.012 mol of NaCl.

in TiACH pillars to 17.7–18.6 Å for TiO_2-pillared clays. Sterte (25) has also reported the interlayer spacing of TiO_2-crosslinked montmorillonite to be about 18 Å. ACH-pillared clays with spacings of about 10 Å were reported by Lahov et al. (30) and Yamanaka and Brindley (31).

The difference between the basal spacing obtained from the TiO_2 and TiACH-pillared clay can be attributed to the larger cationic entities formed (25, 32) from $TiCl_4$ compared to those from the Al-containing cations (21). The pillaring process for the Al_{13} polymer has been investigated by Fripiat and co-workers (21). They report that the uptake of the Al_{13} pillaring species is highly dependent on the net cationic charge of the species. This will vary between 4^+ and 7^+ depending on the number of OH^- or H_2O species in the aluminum octahedra. Monomeric aluminum species in equilibrium with Al_{13} in the aluminum hydroxide solution are preferentially intercalated due to lower steric hindrance within the interlamellar space (21). As

intercalation proceeds the anions coordinated to the Al_{13} species are removed. Upon heating, the Al_{13} species form a metal–oxide pillar.

Titania pillars in TiO_2-pillared clays are produced by the partial hydrolysis of $TiCl_4$ in HCl which causes polymerization of Ti cations (25). The extent of this polymerization depends on the Cl^- and Ti^{4+} concentrations. Einga has proposed that the polynuclear cationic species $((TiO)_8(OH)_{12})^{4+}$ is formed (32) during hydrolysis. These species are linked together by Cl^- bridges. Further hydrolysis to TiO_2 occurs during exchange. Sterte reports that typical uptake by montmorillonite clays results in 10 mmol Ti/g clay (25).

B. X-Ray Diffraction of Synthetic Titania

Amorphous titania was also synthesized by Wright and co-workers (26) via TiO_2 gel formed by hydrolyzing titanium isopropoxide in an acidic solution. The mechanism of titanium hydrolysis has been studied and reviewed by Barksdale (33). In the first step

a hydroxyl ion binds to a titanium ion, thereby lowering the positive charge on the complex by 1 unit. Further reaction results in loss of complexing water and the combination of 2 such units bridged through hydroxyl groups. Further loss of protons and water combined with additional bridging forms chains and crosslinked complexes. These complexes grow until they reach colloidal size whereupon precipitation of an insoluble hydrous titanium oxide begins. Heating of this product produces anatase at 375°C or rutile at 850°C.

C. Surface Area Measurements

As is evident from Table 1, pillaring increases the specific surface area and the interlamellar spacing of clays. Clay pillared by TiO$_2$ has the largest surface area and the greatest increase in basal spacing as indicated by X-ray diffraction. Clays synthesized with TiACH pillars have slightly lower surface areas than those of TiO$_2$-pillared clays. The surface areas reported here may be compared with surface areas of 300–500 m^2/g for aluminum, zirconium, and aluminum–zirconium-pillared clays reported by Occelli (34). Iron–ACH-pillared clays have been reported to have surface areas ranging from 95 to 130 m^2/g (38). The same observation can be made for the TiACH-pillared clay. Yamanaka and co-workers (22) and Sterte (25) report surface area measurements on TiO$_2$-pillared clays ranging from 200 to 350 m^2/g. As seen from Table 1, heating synthetic titania lowers its surface area, probably due to crystal growth or polymorphism.

D. EPR Spectroscopy

Similar EPR spectra have been previously reported by Anpo and co-workers (35). They observed that $g_1 = 2.014_6$ and $g_2 = 2.003_2$ for small TiO$_{2-x}$ particles. They also report a signal with a g-value of 1.988 and attributed it to the formation of Ti^{3+} ions upon irradiation. Our hydrated materials display EPR spectra with similar characteristics.

E. Dichloromethane Photocatalysis by Clays and Pillared Clays

Figures 2 and 4 summarize the photocatalysis data for the degradation of dichloromethane. Pillared clay catalysts are more active than clay catalysts. Bentolite L not exchanged with titanium ions shows a minimal amount of activity. This is an indication of a slight amount of degradation by light in the absence of the catalytically active species. This amount, however, is inconsequential compared to the degradation produced by inclusion of titania. Titania-pillared clays show more activity than TiACH-pillared clays. The higher degree of activity of the pillared clays (titania-pillared clays in particular) can be directly attributable to the high degree of pillaring as indicated by the BET and X-ray diffraction data. The greater surface area allows for greater interaction between the dichloromethane and the titanium.

The pH data do not show a big difference between reactions catalyzed by clays or by pillared clays. In the presence of a titanium catalyst other reactions occur in water such as the generation of hydrogen peroxide (36). With side reactions occurring along with the dichloromethane degradation, it would be difficult to sort out the effects of pH on catalytic reactions (37–40).

F. Synthetic Titania Photocatalysis

Photocatalysis results indicate synthetic, amorphous titania is a less active catalyst than rutile, especially when initial rates are compared on a unit surface area basis. The rutile catalysts, in fact, is the most active of any sample studied. An explanation of this behavior could lie in the availability of active sites for adsorption on this rutile catalyst. If this modification favors adsorption of the dichloromethane then the catalyst–reactant contact will be increased and a greater amount of degradation will result.

G. Dichloromethane Degradation Mechanism

Ollis and co-workers investigated the photocatalytic degradation of simple chlorohydrocarbons by TiO_2 catalysts (5-9). They considered two mechanisms for the initial step of dichloromethane adsorption (6). In one model dichloromethane adsorbs by reacting with a hole on the TiO_2 surface. In the other the chlorocarbon molecule donates a proton to the lattice oxygen of the catalyst and the resulting chlorocarbon anions attach to a titanium cation in the lattice. The latter mechanism is supported by experimental data (6) which indicate that H^+ from HCl competes with H^+ abstraction from the chlorocarbon molecule. The former mechanism is suggested by our preirradiation data.

H. Preirradiation of Catalysts

Preirradiating pillared clays and titania catalysts increases their catalytic activity. This effect may arise from the formation of electron-hole pairs which act as catalytic sites on the TiO_2. During preirradiation these sites increase in number without poisoning by chloride ions.

I. Role of Oxygen

The increased reaction rate caused by bubbling oxygen is consistent with the overall stoichiometry given as

$$CH_2Cl_2 + O_2 \rightarrow 2HCl + CO_2$$
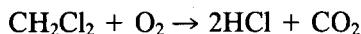
The fact that some activity persists even after oxygen is removed from the reaction mixture suggests that lattice oxygen may also play a role in the reaction.

J. Poisoning and Reusability Studies

The data indicate the catalyst is deactivated by chloride ion and that some activity can be partially restored by washing deactivated catalysts in water. Catalyst activity is also markedly decreased when exogenous NaCl is added to the reaction mixture. Chloride ions may compete with dichloromethane during the first catalytic adsorption step. Rutile is most susceptible to poisoning by Cl^-, consistent with its lower specific surface area.

K. Effect of pH

Table 2 indicates greater catalyst resistance to deactivation and greater initial rates of reaction at lower pH, a curious behavior because degradation of dichloromethane produces HCl as a reaction product. Increasing the basicity could favor hydrogen peroxide formation from OH^-, a reaction that could compete for photons with the reaction for degradation of CH_2CL_2.

V. CONCLUSION

Synthetic rutile was the most active catalyst for photodecomposition of dichloromethane followed by anatase and amorphous titania. Clays pillared by titania are more catalytically active than clays pillared by aluminum polyoxocations or clays containing titanium at exchangeable sites. TiO_2 catalysts (other than rutile) have also been supported on carbon felt. This allows easy separation of the catalyst from the reaction mixture. All of these catalysts can be made more active by oxygen enrichment of the reaction solution or preirradiating the catalyst with light.

REFERENCES

1. Helz, G. R., and Kosak-Channing, L., Environ. Sci. Technol. 2, 48A (1984).
2. Alben, K., and Shpirt, E., Environ. Sci. Technol. 17(4), 187 (1983).
3. Schwarzenbach, R. P., Molnar-Kubica, E., Giger, W. and Wakeham, S. G., Environ. Sci. Technol. 13, 367 (1979).
4. Oliver, B. G. and Nicol, K. D., Environ. Sci. Technol. 16(8), 532 (1982).
5. Ollis, D. F., and Pruden, A. L., J. Catal. 82, 404 (1983).

6. Ollis, D. F., Hsiao, C.-Y., and Lee, C.-L., *J. Catal.* **82,** 418 (1983).

7. Ollis, D. F., and Pruden, A. L., *Environ. Sci. Technol.* **17,** 628 (1983).

8. Ollis, D. F., and Altmed, S., *Sol. Energy* **32,** 597 (1984).

9. Ollis, D. F., Hsiao, C.-Y., Budiman, L., and Lee, C.-L., *J. Catal.* **88,** 89 (1984).

10. Suib, S. L., and Carrado, K. A., *Inorg. Chem.* **24,** 863 (1985).

11. Suib, S. L., Tanguay, J. F., and Occelli, M. L., *J. Amer. Chem. Soc.* **108,** 6972 (1986).

12. Pinnavia, T. J., *Science,* 365 (1983).

13. Laszlo, P., *Science,* 1473 (1987).

14. Theng, B. K. G., *in* "Developments in Sedimentology" (H. Van Olphan, and F. Veniale, Eds.), Vol. 35. Elsevier, Amsterdam, 1982.

15. Yamanaka, S., Doi, T., Sako, S., and Hattori, M., *Mater. Res. Bull.* **19,** 161 (1984).

16. Pinnavaia, T. J., Tzou, M-S., and Landau, S. D., *J. Amer. Chem. Soc.* **107,** 4783 (1985).

17. Occelli, M. L., and Tindwa, R. M., *Clays Clay Miner.* **31,** 22 (1983).

18. Carrado, K. A., Suib, S. L., Skoularikis, N. D., and Coughlin, R. W., *Inorg. Chem.* **25,** 4217 (1986).

19. Carrado, K. A., Kostapapas, A., Suib, S. L., and Coughlin, R. W., *Solid State Ionics* **22,** 117 (1986).

20. Burch, R., and Warburton, C. I., *J. Catal.* **97,** 503 (1986).

21. Plee, D., Gatineau, L., and Fripiat, J. J., *Clays Clay Miner.* **35,** 81 (1987).

22. Yamanaka, S., Nishihara, T., and Hattori, M., *Mater. Chem. Phys.* **17,** 87 (1987).

23. Burch, R., and Warburton, C. I., *J. Chem. Soc. Chem. Commun.,* 117 (1987).

24. Rausch, W., and Bale, H. D., *J. Chem. Phys.* **40,** 3891 (1964).

25. Sterte, J., *Clays Clay Miner.* **34,** 658 (1986).

26. Wright, A. F., Mikherjee, S. P., and Epperson, J. E., *J. Phys.* **8,** 521 (1985).

27. Fischer, R. B., and Peters, D. G., "Quantitative Chemical Analysis." Saunders, Philadelphia, 1968.

28. Grim, R. E., "Clay Minerology." McGraw–Hill, New York, 1953.

29. Kuznicki, S. M., DeVries, K. L., and Eyring, E. M., *J. Phys. Chem.* **84,** 535 (1980).

30. Lahov, H., Shani, V., and Shabtai, J., *Clays Clay Miner.* **26,** 107 (1978).

31. Yamanaka, S., and Brindley, G. W., *Clays Clay Miner.* **27,** 119 (1979).

32. Einga, H., *J. Chem. Soc. Dalton. Trans.,* 1917 (1979).

33. Barksdale, J., "Titanium: Its Occurrence, Chemistry, and Technology." Ronald Press, New York, 1949.

34. Occelli, M. L., *In* "Proceedings, Eighth Inter. Clay Conf., 1987" (L. G. Schultz, H. Van Olphen, and F. A. Mumpton, Eds.). Clay Minerals Soc., Inc., 1987.

35. Anpo, M., Shima, T., and Kubokawa, Y., *Chem. Lett.* 1799 (1985).

36. Rives-Arnau, V., *J. Electroanal. Chem.* **190,** 279 (1985).

37. Anderson, J. R., "Structure of Metallic Catalysts." Academic Press, New York, 1975.

38. Kostapapas, A., Ph.D. dissertation, University of Connecticut, Storrs, 1987.

39. Tanguay, J. F., Ph.D. dissertation, University of Connecticut, Storrs, 1988.

40. Barrer, R. M., and MacLeod, D. M., *Trans. Faraday Soc.* **51,** 1290 (1955).